Faraday Discussions

Cite this: *Faraday Discuss.*, 2015, **178**, 421

PAPER

View Article Online
View Journal | View Issue

Optical forces in nanoplasmonic systems: how do they work, what can they be useful for?

T. V. Raziman, R. J. Wolke and O. J. F. Martin*

Received 17th November 2014, Accepted 24th November 2014
DOI: 10.1039/c4fd00224e

In this article, we share our vision for a future nanofactory, where plasmonic trapping is used to control the different manufacturing steps associated with the transformation of initial nanostructures to produce complex compounds. All the different functions existing in a traditional factory can be translated at the nanoscale using the optical forces produced by plasmonic nanostructures. A detailed knowledge of optical forces in plasmonic nanostructures is however essential to design such a nanofactory. To this end, we review the numerical techniques for computing optical forces on nanostructures immersed in a strong optical field and show under which conditions approximate solutions, like the dipole approximation, can be used in a satisfactory manner. Internal optical forces on realistic plasmonic antennas are investigated and the reconfiguration of a Fano-resonant plasmonic system using such internal forces is also studied in detail.

1 Introduction

Since the first observation by Ashkin in 1970 of the acceleration and trapping with optical radiation pressure of freely suspended micron-sized particles,[1] and the demonstration 15 years later by the same author of stable optical trapping in three dimensions using a single-beam gradient optical trap,[2] optical forces produced by a laser beam have been both extensively studied theoretically and applied for contactless manipulation of a broad variety of small objects, especially biological entities, for which optical tweezers have become routine. The following review articles provide an overview of this field of research.[3–6]

The mechanisms of optical trapping can be easily understood – even within the framework of ray optics – if one assumes that each photon forming the optical ray carries some momentum. This is illustrated in Fig. 1, inspired by one of the seminal papers of Ashkin.[2] A dielectric sphere placed in a homogeneous optical field will mainly feel a scattering force that pushes it along

Nanophotonics and Metrology Laboratory, Swiss Federal Institute of Technology Lausanne (EPFL), CH-1015 Lausanne, Switzerland. E-mail: olivier.martin@epfl.ch; Fax: +41 21 693 26 14; Tel: +41 21 693 26 07

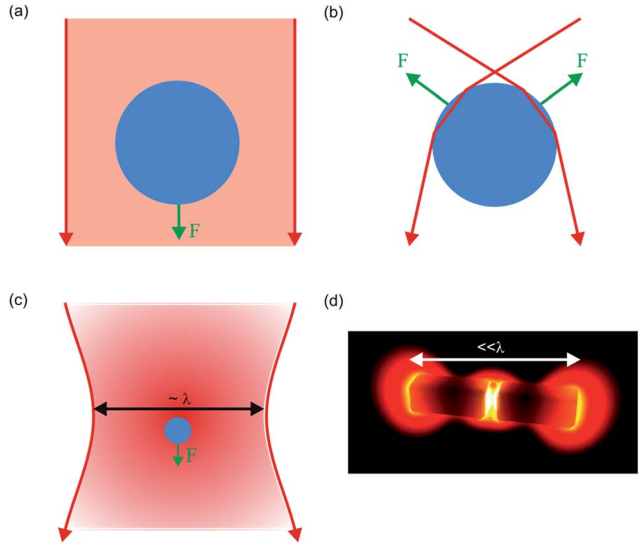

Fig. 1 Different optical trapping configurations. (a) In a homogeneous field, a particle is just pushed along by the scattering force. (b) In the focus of a strong lens, the gradient forces can laterally trap and catch the particle; these forces can be understood in the framework of ray optics, assuming that momentum is transferred from the incoming ray to the sphere at each reflexion or refraction. (c) In far-field optics, the focus produced by a lens is limited to about the wavelength λ; consequently, a very small particle does not "feel" the gradient forces and is merely pushed along by the scattering force. (d) A plasmonic nanostructure can produce extremely strong field gradients, which are not limited by the illumination wavelength, but simply determined by the geometrical features of the nanostructure. In that case, extremely small particles can be trapped near the gap of a plasmonic dipole antenna.

and is not much use for manipulating the sphere, Fig. 1(a). When the same sphere is placed in a strongly focused light beam, the lateral variations of the optical field now also give rise to lateral trapping forces – so called gradient forces – which can be used to trap and manipulate the sphere, Fig. 1(b). The dimensions of this strong focus produced by far-field optics are comparable to the wavelength of radiation used to illuminate the system. Hence, when the sphere becomes much smaller than the wavelength, it does not feel anymore the lateral field gradient and cannot be trapped, Fig. 1(c). This limitation can be overcome by using the very strong field gradient that is produced in the near-field of a plasmonic nanostructure, Fig. 1(d). Hence, in that case, it is possible to trap extremely small objects. It is actually a feature of the near-field that it can be confined to dimensions that are determined by the size of the object that produces the near-field, irrespective of the illumination wavelength.[7] This effect is dramatically intensified in plasmonic nanostructures, where the very strong near-field originates from the confinement of polarization charges at the surface of the metal.[8] We refer the reader to the recent review by the group of Romain Quidant for the development of this field of plasmonic trapping and the different geometries where it has been implemented.[9]

In this contribution, we focus on the optical forces produced by such a plasmonic system and enabled by the strongly localized near-field associated with the plasmon resonance. In Sec. 2, we review the physical mechanisms of optical forces and describe the theoretical framework required to analyse them; we also provide some insightful comparisons with the dipole approximation. We then investigate two facets of plasmonic forces: how they can act internally and externally to reconfigure a system. In Sec. 5 we present our vision for a nanofactory, where optical forces are used as the driving mechanism. The paper is summarized in Sec. 6.

2 Modelling optical forces in plasmonic systems

Maxwell's stress tensor

One must resort to Maxwell's equations to go beyond the simple ray optics picture sketched in Fig. 1(b) to describe the forces produced by light on an object.[10] Starting from the Lorentz force $\mathbf{F}$ caused by the electric field $\mathbf{E}$ and the magnetic induction $\mathbf{B}$ on a charged particle q,

$$\mathbf{F} = q(\mathbf{E} + \mathbf{v} \times \mathbf{B}), \tag{1}$$

and using Newton's second law to link the change of momentum $\mathrm{d}\mathbf{P}/\mathrm{d}t$ in the volume under study with the Lorentz force, one obtains Maxwell's stress tensor σ_{ij} in a medium with permittivity ε and permeability μ,

$$\sigma_{ij} = \varepsilon_0\varepsilon E_i E_j + \mu_0\mu H_i H_j - \frac{1}{2}(\varepsilon_0\varepsilon E_k E_k + \mu_0\mu H_k H_k)\delta_{ij} \tag{2}$$

which can be used to compute the optical force on a scatterer with boundary S,

$$\frac{\partial\left(\mathbf{P}_{\mathrm{mech}} + \mathbf{P}_{\mathrm{field}}\right)_i}{\partial t} = \oint_S \sigma_{ij} n_j \mathrm{d}S, \tag{3}$$

where $\mathbf{P}_{\mathrm{mech}}$ and $\mathbf{P}_{\mathrm{field}}$ are the mechanical and electromagnetic momenta and n the outward normal to the surface S. Assuming harmonic electromagnetic fields, one can compute the time-averaged Maxwell stress tensor,

$$\langle\sigma_{ij}\rangle = \frac{1}{2}\Re\left\{\varepsilon_0\varepsilon E_i E_j^* + \mu_0\mu H_i H_j^* - \frac{1}{2}\left(\varepsilon_0\varepsilon E_k E_k^* + \mu_0\mu H_k H_k^*\right)\delta_{ij}\right\}. \tag{4}$$

The time average of the electromagnetic momentum over a period is constant and its derivative in eqn (3) vanishes. Hence, the time averaged optical force acting on the scatterer is given by

$$\langle F_i\rangle = \oint_S \langle\sigma_{ij}\rangle n_j \mathrm{d}S. \tag{5}$$

Numerical implementation

Eqn (5) indicates that the knowledge of the electromagnetic field in the surroundings of a trapped object enables the calculation of the optical force on this object. In practice, the electromagnetic field is first computed on a mesh that

follows a closed surface around the object, usually a sphere (Fig. 2(a)), and the optical force is computed using eqn (5).[11–15] Although this approach involves an additional overhead since a large number of surface points might need to be sampled to compute the optical force accurately, it is perfectly suitable for a variety of geometrical configurations, especially when the different scatterers are placed far apart. It often becomes cumbersome in the case of plasmonic trapping, where the trapped structure is very close to the plasmonic system producing the strong near-field, as illustrated in Fig. 2(b). To overcome this difficulty, we recently proposed an approached based on the surface integral equation (SIE), where the surface of the trapped particle is directly used to compute Maxwell's stress tensor.[16]

In short, we simulate the optical response of plasmonic structures with the SIE formulation, which utilises Green's dyadic function to solve Maxwell's equations in the frequency domain.[17–19] This method offers various advantages over formulations such as finite difference time domain and volume integral equations in terms of being able to model the scatterer surface very well and in the reduction of computational expenses by requiring the discretisation of only the scatterer surface. SIE simulations output the expansion of surface electric and magnetic currents (which correspond to the tangential magnetic and electric fields, respectively) over Rao, Wilton, and Glisson basis functions on the triangles the scatterer surface has been discretised into.[20] Relevant physical quantities such as fields and optical cross sections can be computed from these surface currents.

Maxwell's stress tensor is then directly evaluated over the triangles the scatterer surface has been discretised into, in terms of the surface electric $\mathbf{J}$ and magnetic $\mathbf{M}$ currents without computing the fields explicitly, Fig. 2(b). The expression for the force in terms of the currents over the triangles is

$$\mathbf{F} = \sum_T \int_T \mathrm{d}S_T \left\{ \frac{(\nabla\cdot\mathbf{M})(\nabla\cdot\mathbf{M}^*)}{2\omega^2\mu^*}\hat{\mathbf{n}} + \frac{(\nabla\cdot\mathbf{J})(\nabla\cdot\mathbf{J}^*)}{2\omega^2\varepsilon^*}\hat{\mathbf{n}} + \frac{i}{\omega}\left[\frac{\mu}{\mu^*}(\mathbf{J}\times\hat{\mathbf{n}})(\nabla\cdot\mathbf{M}^*) + \frac{\varepsilon}{\varepsilon^*}(\hat{\mathbf{n}}\times\mathbf{M})(\nabla\cdot\mathbf{J}^*)\right] - \frac{1}{2}(\varepsilon\mathbf{M}\cdot\mathbf{M}^* + \mu\mathbf{J}\cdot\mathbf{J}^*)\hat{\mathbf{n}}\right\}. \quad (6)$$

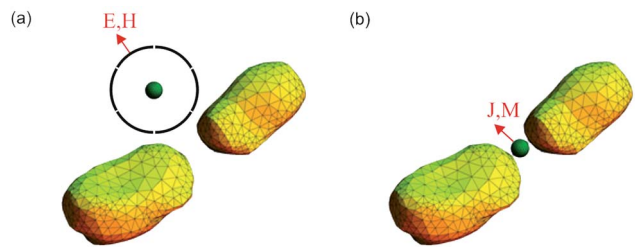

Fig. 2 Calculation of the optical forces on a nanostructure at the vicinity of a plasmonic dipole antenna using Maxwell's stress tensor. (a) In general, a virtual surface (*e.g.* the sphere in black) is defined around the nanostructure and the total electromagnetic field **E**, **H** is computed on that surface. The force on the object is then deduced using eqn (4). This approach is not well suited in the case of intricate trapping geometries, such as those encountered in plasmonic trapping. (b) Recently, we developed an alternative approach, where the optical force is computed with eqn (6) directly from the surface currents **J**, **M** on the trapped particle obtained from the SIE calculation for the complete system (plasmonic trapping antenna + trapped nanostructure).

Since the currents are expanded in terms of Rao, Wilton and Glisson basis functions which are linear over geometric coordinates, the integral over each triangle can be performed analytically, reducing further numerical errors during force computation.

Comparison with approximate solutions

The optical forces on small particles in a non-uniform electric field $\mathbf{E}$ can be approximated by the gradient force given by

$$\langle \mathbf{F} \rangle = \frac{1}{4} \Re\{\alpha\} \nabla \mathbf{E}^2, \tag{7}$$

where α is the dipolar polarisability of the particle under consideration. This approximate solution enables us to reveal another facet of plasmonic trapping, whereby the trapped particle supports plasmon resonances as well. Indeed, for a

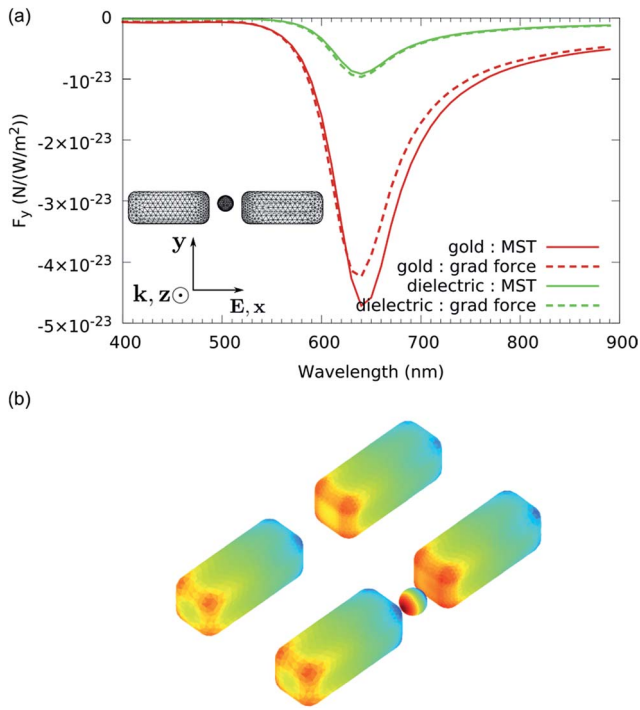

Fig. 3 Restoring forces on a nanoparticle displaced from the centre of a plasmonic gap antenna shown in the inset of (a). The antenna is made of gold with arms of dimensions 100 nm × 40 nm × 40 nm and a gap of 40 nm, and is placed with the antenna axis along x. A spherical particle of 10 nm radius is placed at the centre of the gap and displaced by 5 nm along y. The structure is illuminated by a plane wave propagating along z and polarised along x. (a) Comparison of restoring forces on a particle made of dielectric (glass) and metal (gold), computed using the Maxwell's stress tensor method and using the gradient force approximation. The gradient force method provides a good approximation for the force for the entire wavelength range. (b) Polarisation charges induced on the structure at the peak force wavelength both in the absence of the sphere and when the sphere is present. The presence of the sphere does not modify the charge distribution significantly.

given volume, a plasmonic particle can exhibit a much stronger polarizability than a dielectric particle.[21] This is advantageous in terms of detecting the trapping event,[22] and provides additional degrees of freedom for trapping a plasmonic nanostructure with a plasmonic trap, since the resonance of the coupled system can be fully tuned (from trapping to repelling) depending on the relative energy of both plasmon resonances.[23]

We next look at the applicability of this approximation by comparing it with the SIE results using Maxwell's stress tensor. The system under consideration is a gap antenna with arms of dimensions 100 nm $\times$ 40 nm $\times$ 40 nm made of gold. The antenna is illuminated by a plane wave propagating in the z-direction polarised along x. A sphere is placed at the centre of the gap between the antenna arms and displaced by 5 nm along y, and we look at the restoring force.

Fig. 3(a) shows the comparison between the forces calculated using the gradient force method and the Maxwell's stress tensor method for a gap of 40 nm and the displaced particle of radius 10 nm. We see that the gradient force approach is quite good for both the metallic (gold) particle and the dielectric (glass) particle, though the quantitative agreement is better for the latter. To understand better the reason behind this, we show the polarisation

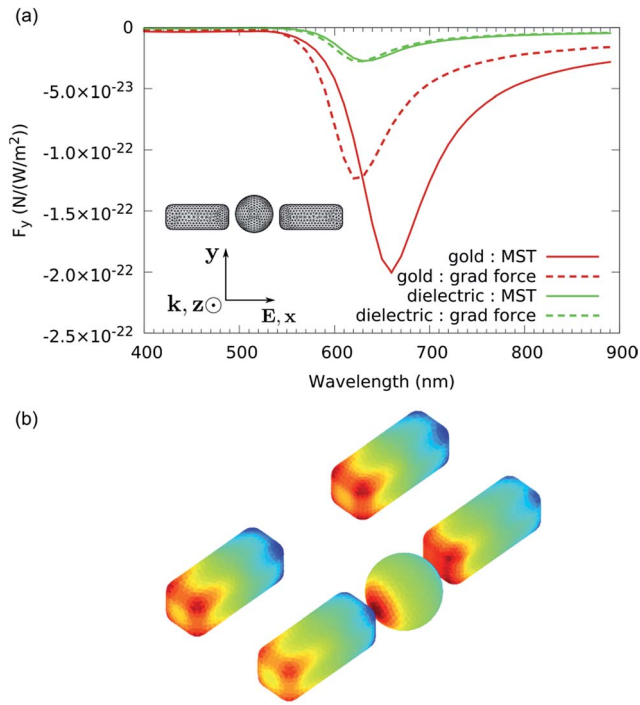

Fig. 4 Restoring forces on a larger nanoparticle of radius 30 nm, placed in a larger gap of 80 nm, as shown in the inset of (a), with other parameters the same as in Fig. 3. (a) Comparison of restoring forces computed using the two methods, showing that the gradient force approximation is now highly inaccurate for the case of the gold particle. (b) Polarisation charges induced on the structure are modified in the presence of the larger sphere, with a significant charge migration towards the gap faces in this case.

charges induced on the scatterer surfaces (calculated directly from the surface currents again) at the peak force wavelength in Fig. 3(b). It can be seen that the presence of the small sphere does not affect the charge distribution significantly, the result of which is that the gradient force calculation, which assumes that the presence of the sphere does not change the field distribution due to the other scatterers, works quite well.

We now repeat the calculation for a larger particle with 30 nm radius placed in an 80 nm gap, Fig. 4(a) shows the force computed using both methods. Though the results for the dielectric particles are quite reasonable, the gradient force shows a large mismatch with the Maxwell's stress tensor method for the metallic particle. The induced polarisation charges plotted in Fig. 4(b) explain why this happens. The inclusion of the large spherical particle affects the charge distribution on the antenna arms considerably, in particular, attracting the surface charges towards the gap faces. As a result, the electric field in the gap due to the arms changes a lot. Also, the electric field varies quite significantly over the dimensions of the particle unlike in the previous case. Consequently, the gradient force method is inadequate for force calculations in that case. Such behaviour even for particles quite smaller than the wavelength of light (at peak force wavelength, the gold sphere diameter is less than one-tenth the wavelength) shows the importance of using full Maxwell's stress tensor calculations for forces in plasmonic systems.

3 Internal forces in plasmonic systems

The vast majority of works reported on the transfer of momentum from an external field onto a nanostructure consider how the external field can modify the motion of the nanostructure. To the best of our knowledge, internal forces within the nanostructure induced by an external field have not yet been touched upon. Here, we look at the optical forces on the realistic gap antenna shown in the inset of Fig. 5(a), which discretization has been obtained from a fabricated structure.[24] The antenna is made out of gold, with arms of approximate dimensions 110 nm $\times$ 50 nm $\times$ 50 nm, and the gap between the antenna arms is approximately 20 nm. The gap antenna is illuminated by an x-polarised plane wave propagating in the z-direction. The scattering cross section for the structure as a function of the wavelength is shown in Fig. 5(a). The dipolar resonance of the gap antenna results in a strong scattering peak at 630 nm.

Fig. 5(b) shows the optical forces on the arms of the gap antenna. Clearly, the arms of the antenna attract each other throughout the wavelength range under consideration. Also, both arms are pushed in the z-direction due to the scattering force. Interestingly, we note that the pushing forces on the two arms are not identical due to the realistic and non-identical nature of the arms. Even the x-forces on the arms are not exactly equal in magnitude. In fact, there is also a small force on the arms in the y-direction (not shown in figure), again a consequence of the realistic and asymmetric nature of the structure.

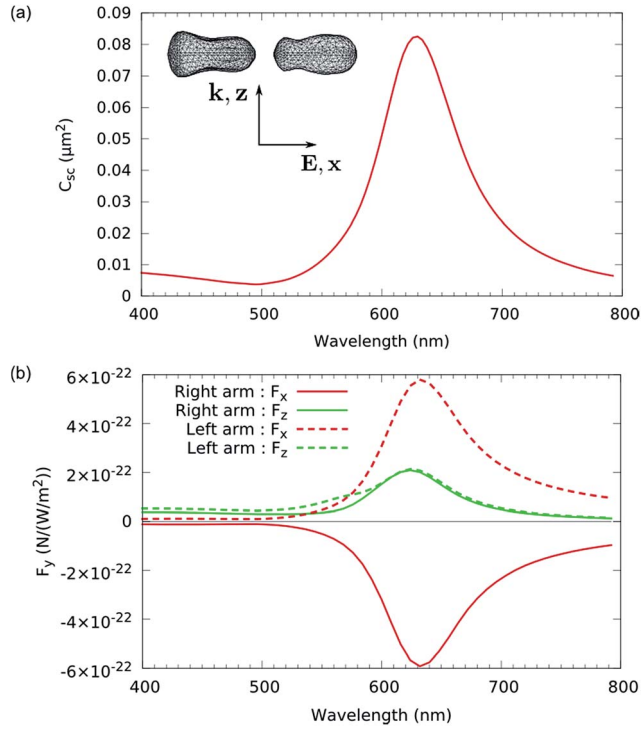

Fig. 5 Optical forces on a realistic gap antenna made of gold, shown in the inset of (a). The antenna is placed with the long axis along *x*, and illuminated by an incident plane wave propagating along *z* and polarised along *x*. (a) Scattering cross section of the antenna, showing the dipolar resonance peak near 630 nm. (b) Scattering force (along *z*) and internal force (along *x*) on the arms of the antenna. The realistic, asymmetric geometry results in unequal forces on the two arms.

4 Reconfiguring plasmonic systems using optical forces

The integration of nano-optical traps into a plasmonic system allows for a new type of reconfigurable plasmonic devices by utilizing the interaction between the trap and the trapped particle. Using specifically designed plasmonic nanostructures, the optical forces can be tailored to accommodate plasmonic colloidal particles at locations critical to the spectral response of the complete system.

Of particular interest are switchable Fano resonances, due to the large and broadband spectral variation that is not limited to spectral shifts or the creation of additional modes.[25–28] Furthermore, the strong field enhancements typical for the subradiant mode of a Fano resonance give rise to particularly strong optical forces. Under resonant laser excitation, the potential energies associated with these forces exceed those of Brownian motion, creating a potential well deep enough to trap particles at room temperature.

An example of such a system is heptamers of plasmonic discs. In the absence of the central particle, the ring-like hexamer exhibits a dipolar mode. Adding a

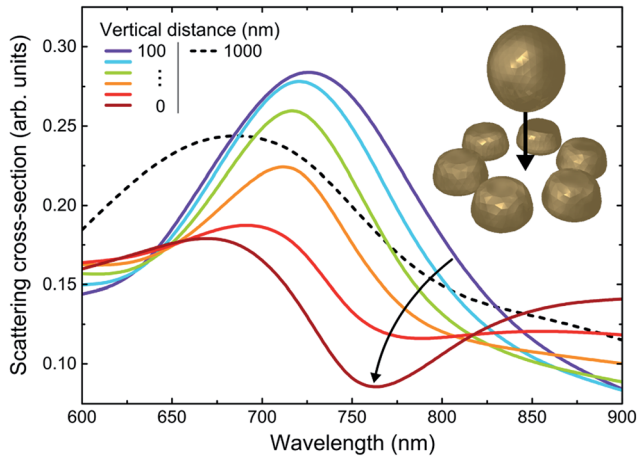

Fig. 6 Calculated scattering cross-section spectra of a hexamer of gold nanodiscs (d = 120 nm, h = 60 nm) in the presence of a gold sphere (r = 75 nm) located above the center of the structure, illuminated by a linearly polarized plane wave under normal incidence. Spectra are shown for different vertical distances of the sphere as measured from the bottom of the sphere to the bottom of the discs. As the sphere approaches the center of the hexamer (solid lines, top to bottom), a Fano resonance appears in the spectrum around 760 nm, due to the coupling between the hexamer's ring-like mode and the now supported linear mode. The dashed black line shows the uncoupled system, represented by placing the sphere 1 μm above the hexamer.

seventh particle in the center of the ring leads to the addition of linear modes to the system. More importantly, the coupling of ring-like and linear modes can lead to a Fano resonance. The spectral behavior of the plasmonic heptamer can be preserved when substituting the central disc by a spherical particle of similar size, making it an ideal candidate for a reconfigurable plasmonic system based on optical trapping of colloidal plasmonic nanospheres.

Fig. 6 shows SIE simulations of the scattering intensity of a gold hexamer that can be used for trapping. Included in the simulations is a gold sphere, positioned at different heights above the centre of the hexamer, ranging from 0 to 100 nm above the substrate (not included in the simulation), as indicated by the legend. As the sphere lowers into the trap, the spectrum changes and a distinct Fano resonance appears, with a subradiant mode around 760 nm for a distance of 0 (dark red line). The dotted line shows the combined spectrum of the hexamer and sphere without coupling, by placing the sphere at a height of 1 μm. The spectral responses for the two extreme cases are fundamentally different and easily distinguishable over a broad wavelength range.

5 Optical forces as drivers for a nanofactory

In this section, we would like to share our vision for realizing at the nanoscale the equivalent of a factory where structures are engineered through successive transformation steps. While, in the industrial revolution era, the different machineries operated in a factory would take their energy from a rather

sophisticated line shaft, we propose that most of the operations required by such a nanofactory could be controlled with optical forces, as illustrated in Fig. 7.

As in a conventional factory, the first step is to move the new material to the location where it should be processed, Fig. 7(a). This can be achieved using the optical forces generated by surface plasmon polaritons propagating on a gold

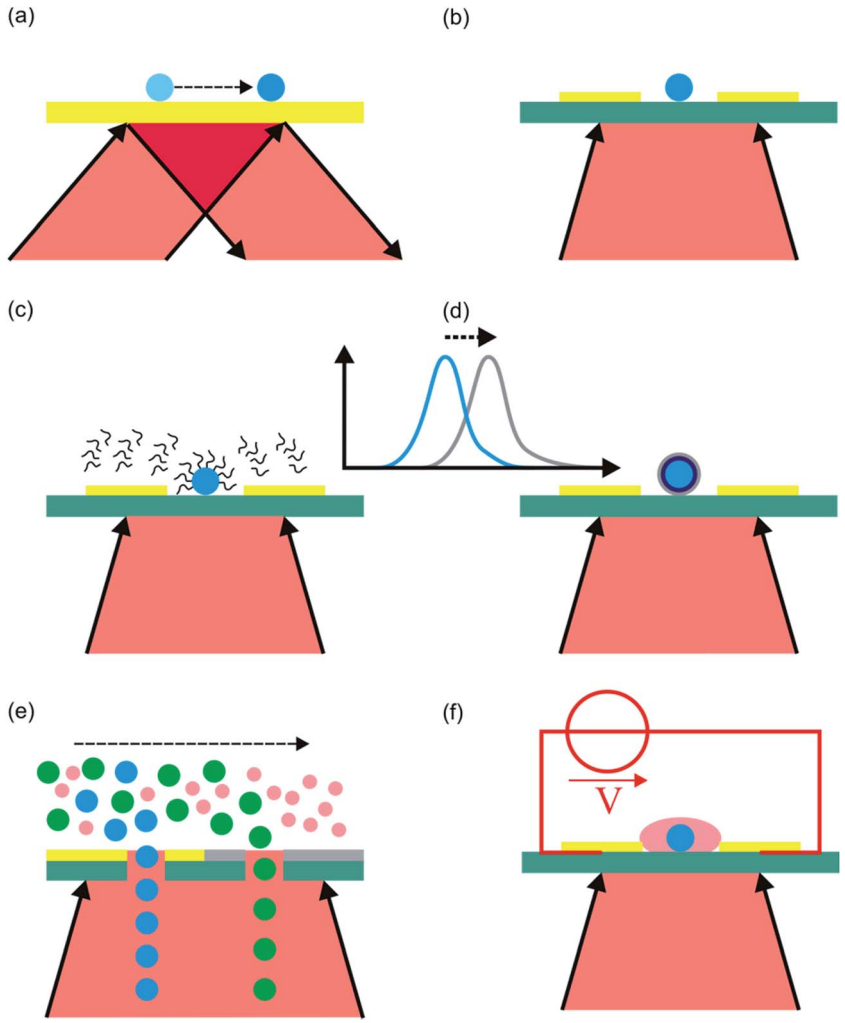

Fig. 7 The different manufacturing steps required for a nanofactory, where incoming nanostructures are modified and engineered into more complex products, can be controlled with plasmonic forces. (a) Plasmonic conveyor belt to move incoming nanostructures into position. (b) Immobilization of a nanostructure into its position. (c) Surface functionalization using chemistry to modify the nanostructure's surface. (d) Adjunction of new materials onto the nanostructure. Both processes can be monitored through the evolution of the spectral response of the nanostructure. (e) Sorting of final products or waste using a plasmonic sieve. (f) Additional manufacturing functions could be obtained by combining optical forces with electromagnetic fields applied directly onto the nanostructure under fabrication.

film.[29–31] Even in the simplest Kretschmann configuration, where a surface plasmon is excited by illumination through a prism, a standing plasmon can be produced on the surface of the metal. By controlling the phase of this standing wave, nanostructures can be moved along in a very controlled manner. For asymmetric trapped nanostructures, this approach can also be used to orient the nanostructure along a specific direction using the incident polarization.[32]

The nanostructure to be worked upon should then be immobilized. This can be performed using plasmonic trapping at the vicinity of a plasmonic antenna, Fig. 7(b). It could also be achieved using a reconfigurable structure, like that discussed in Sec. 4. Monitoring the optical response of the trapping structure provides means of following the immobilization of the trapped nanostructure, even when this structure is extremely small.[33] It should be mentioned that we assume that the entire nanofactory relies on microfluidics to bring in additional components or eliminate by-products.[34]

Once the nanostructure has been immobilized at a specific location, it can be worked upon. For example, specific surface chemistry can be used to functionalize its surface, Fig. 7(c). This surface functionalization can provide a broad variety of new functions,[35,36] that can be used for further nano-assembly[37] or to design a final product for specific applications, *e.g.* in biology.[38] Surface functionalization can be brought even further, by completely modifying the original nanostructure, Fig. 7(d). A typical example is that of the creation of multi-layered nanostructures, such as core–shell particles,[39] which broaden the possible optical responses for such nanostructures. Novel materials, like organic semiconductors, can also be combined with the carrying nanostructure to expand the range of possible applications, *e.g.* toward photovoltaics.[40]

For both surface functionalization and nanostructure modification, the evolution of the process can be followed in real time by monitoring the spectral changes in the optical response of the nanostructure (see the inset in Fig. 7). Especially for plasmonic nanostructures, minute variations of the geometry resulting from adsorption or aggregation, produce very noticeable modifications of the spectrum. This unique feature of a nanofactory driven by plasmonic forces enables extremely accurate control of the different steps required for the production of complex aggregates.

If the nanofactory relies on microfluidics to incorporate new components and eliminate waste or final products, a sorting step can be mandatory. This step can be required to sort between waste and final products, or to sort final products depending on their characteristics. This manufacturing step can easily be implemented with plasmonic trapping using a membrane and the extraordinary optical transmission phenomenon, Fig. 7(e).[9,41] Different degrees of freedom can be used here: the type of metal used – which determines the surface modes that can be excited and can dictate which particle will be selected, Fig. 7(e); the geometry of the apertures – which determines the resonances in the corresponding cavity; the surface chemistry – which can be used to selectively allow the passage of specific nanostructures.

So far, this foreseen nanofactory has used a combination of optical forces and surface chemistry to modify an original nanostructure and produce a more advanced system. It is very likely that in the future, the integration of electrical functions with such a system will provide further degrees of freedom, Fig. 7(f). By either directly contacting the nanostructure under work,[42] or immersing it in a

very strong electromagnetic field, additional functionalities will be possible, including the specific growth of the structure by electrophoresis.[43] The combination of this approach with semiconductor nanomaterials will broaden even further the scope of possibilities for such a nanofactory.[44]

6 Summary

We have reviewed the numerical techniques for computing optical forces on nanostructures immersed in a strong optical field. In particular, we have shown that a recently introduced method that combines the surface integral equation with Maxwell's stress tensor is particularly well suited for computing optical forces produced by plasmonic structures on particles trapped at their ultimate vicinity. This fully electromagnetic approach has been compared with the dipole approximation for gradient forces calculations. While for specific geometries where the trapped object does not disturb much the illumination field, this approximation gives good results; however, it rapidly fails as soon as the interaction between the trapped particle and the structure producing the near-field becomes significant. Our data indicate that this is already the case for trapped particles as small as one tenth of the wavelength.

Studying a realistic optical antenna, we have shown that upon external illumination, both arms of the antenna undergo attractive optical forces. Due to the realistic shape of the structure, these forces are non-symmetrical, resulting in a torque on the overall structure. These internal forces are more complex for a nanostructure that includes several parts, as is the case for the heptamer that we have investigated. In that case, the seventh particle can be trapped in the centre of the structure, to complete its geometry. Upon trapping, we have observed very significant changes in the response of the system, especially the Fano resonance associated with such a structure can be fully controlled by the plasmonic trapping of one single nanoparticle.

Finally, we have shared our vision of a future nanofactory, where plasmonic trapping is used to control the different manufacturing steps associated with the transformation of initial nanostructures to produce complex compounds. All the different functions existing in a traditional factory can be translated at the nanoscale using the optical forces produced by plasmonic nanostructures.

Acknowledgements

Funding from the Swiss National Science Foundation (grant 200020_135452) is gratefully acknowledged.

References

1 A. Ashkin, *Phys. Rev. Lett.*, 1970, **24**, 156–159.
2 A. Ashkin, J. M. Dziedzic, J. E. Bjorkholm and S. Chu, *Opt. Lett.*, 1986, **11**, 288–290.
3 D. G. Grier, *Nature*, 2003, **424**, 810–816.
4 J. R. Moffitt, Y. R. Chemla, S. B. Smith and C. Bustamante, *Annu. Rev. Biochem.*, 2008, **77**, 205–228.
5 K. C. Neuman and S. M. Block, *Rev. Sci. Instrum.*, 2004, **75**, 2787–2809.

6 M. Woerdemann, C. Alpmann, M. Esseling and C. Denz, *Laser Photonics Rev.*, 2013, **7**, 839–854.
7 O. J. F. Martin, C. Girard and A. Dereux, *Helv. Phys. Acta*, 1995, **68**, 195–196.
8 J. P. Kottmann, O. J. F. Martin, D. R. Smith and S. Schultz, *New J. Phys.*, 2000, **2**, 27.
9 M. L. Juan, M. Righini and R. Quidant, *Nat. Photonics*, 2011, **5**, 349–356.
10 J. D. Jackson, *Classical Electrodynamics*, Wiley, 3rd edn, 1998.
11 P. C. Chaumet and M. Nieto-Vesperinas, *Phys. Rev. B: Condens. Matter Mater. Phys.*, 2001, **64**, 035422.
12 D. Ganic, X. Gan and M. Gu, *Opt. Express*, 2004, **12**, 2670–2675.
13 M. L. Povinelli, M. Loncar, M. Ibanescu, E. J. Smythe, S. G. Johnson, F. Capasso and J. D. Joannopoulos, *Opt. Lett.*, 2005, **30**, 3042–3044.
14 E. Lamothe, G. Lévêque and O. J. F. Martin, *Opt. Express*, 2007, **15**, 9631–9644.
15 J. Chen, J. Ng, Z. F. Lin and C. T. Chan, *Nat. Photonics*, 2011, **5**, 531–534.
16 A. Ji, T. V. Raziman, J. Butet, R. P. Sharma and O. J. F. Martin, *Opt. Lett.*, 2014, **39**, 4699–4702.
17 M. Paulus and O. J. F. Martin, *Opt. Quantum Electron.*, 2001, **33**, 315–325.
18 A. M. Kern and O. J. F. Martin, *J. Opt. Soc. Am. A*, 2009, **26**, 732–740.
19 B. Gallinet, A. M. Kern and O. J. F. Martin, *J. Opt. Soc. Am. A*, 2010, **27**, 2261–2271.
20 S. Rao, D. Wilton and A. Glisson, *IEEE Trans. Antennas Propag.*, 1982, **30**, 409–418.
21 C. F. Bohren and D. R. Huffman, *Absorption and Scattering of Light by Small Particles* 1983.
22 A. Lovera and O. J. F. Martin, *Appl. Phys. Lett.*, 2011, **99**, 151104.
23 L. Huang and O. J. F. Martin, *Opt. Lett.*, 2008, **33**, 3001–3003.
24 A. M. Kern and O. J. F. Martin, *Nano Lett.*, 2011, **11**, 482–487.
25 B. Luk'yanchuk, N. I. Zheludev, S. A. Maier, N. J. Halas, P. Nordlander, H. Giessen and C. T. Chong, *Nat. Mater.*, 2010, **9**, 707–715.
26 B. Gallinet and O. J. F. Martin, *Phys. Rev. B: Condens. Matter Mater. Phys.*, 2011, **83**, 235427.
27 B. Gallinet and O. J. F. Martin, *Opt. Express*, 2011, **19**, 22167–22175.
28 A. Lovera, B. Gallinet, P. Nordlander and O. J. F. Martin, *ACS Nano*, 2013, **7**, 4527–4536.
29 G. Volpe, R. Quidant, G. Badenes and D. Petrov, *Phys. Rev. Lett.*, 2006, **96**, 238101.
30 D. B. Ruffner and D. G. Grier, *Phys. Rev. Lett.*, 2012, **109**, 163903.
31 O. Brzobohatý, V. Karásek, M. Šiler, L. Chvátal, T. Čižmár and P. Zemánek, *Nat. Photonics*, 2013, **7**, 123–127.
32 Y. Zhang, J. Wang, J. Shen, Z. Man, W. Shi, C. Min, G. Yuan, S. Zhu, H. P. Urbach and X. Yuan, *Nano Lett.*, 2014, **14**, 6430–6436.
33 W. Zhang, L. Huang, C. Santschi and O. J. F. Martin, *Nano Lett.*, 2010, **10**, 1006–1011.
34 L. Huang, S. Maerkl and O. J. F. Martin, *Opt. Express*, 2009, **17**, 6018–6024.
35 R. A. Sperling and W. J. Parak, *Philos. Trans. R. Soc. London, Ser. A*, 2010, **368**, 1333–1383.
36 R. Mout, D. F. Moyano, S. Rana and V. M. Rotello, *Chem. Soc. Rev.*, 2012, **41**, 2539–2544.
37 W. Li, P. H. C. Camargo, X. Lu and Y. Xia, *Nano Lett.*, 2009, **9**, 485–490.

38 A. Verma, O. Uzun, Y. Hu, Y. Hu, H.-S. Han, N. Watson, S. Chen, D. J. Irvine and F. Stellacci, *Nat. Mater.*, 2008, **7**, 588–595.
39 S. J. Oldenburg, R. D. Averitt, S. L. Westcott and N. J. Halas, *Chem. Phys. Lett.*, 1998, **288**, 243–247.
40 R. Plass, S. Pelet, J. Krueger, M. Grätzel and U. Bach, *J. Phys. Chem. B*, 2002, **106**, 7578–7580.
41 H. J. Lezec, A. Degiron, E. Devaux, R. A. Linke, L. Martin-Moreno, F. J. Garcia-Vidal and T. W. Ebbesen, *Science*, 2002, **297**, 820–822.
42 E. C. Garnett, W. Cai, J. J. Cha, F. Mahmood, S. T. Connor, M. Greyson Christoforo, Y. Cui, M. D. McGehee and M. L. Brongersma, *Nat. Mater.*, 2012, **11**, 241–249.
43 F. Iwata, M. Kaji, A. Suzuki, S. Ito and H. Nakao, *Nanotechnology*, 2009, **20**, 6.
44 M. Heiss, Y. Fontana, A. Gustafsson, G. Wüst, C. Magen, D. D. O'Regan, J. W. Luo, B. Ketterer, S. Conesa-Boj, A. V. Kuhlmann, J. Houel, E. Russo-Averchi, J. R. Morante, M. Cantoni, N. Marzari, J. Arbiol, A. Zunger, R. J. Warburton, A. Fontcuberta and I. Morral, *Nat. Mater.*, 2013, **12**, 439–444.

